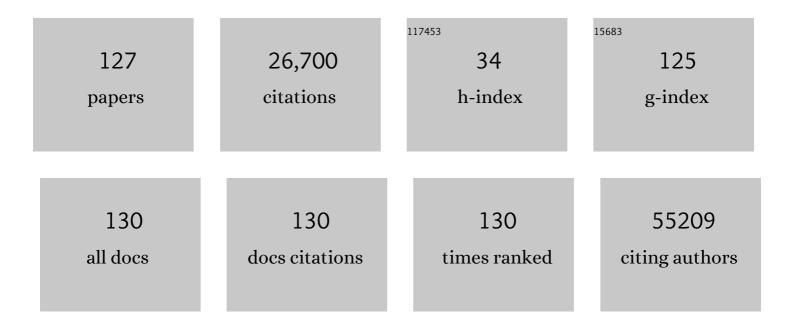
List of Publications by Year in descending order

Source: https://exaly.com/author-pdf/5874198/publications.pdf Version: 2024-02-01



#	Article	IF	CITATIONS
1	Development and Validation of Noninvasive <scp>MRI</scp> â€Based Signature for Preoperative Prediction of Early Recurrence in Perihilar Cholangiocarcinoma. Journal of Magnetic Resonance Imaging, 2022, 55, 787-802.	1.9	16
2	Dataâ€Driven Modification of the <scp>Llâ€RADS</scp> Major Feature System on Gadoxetate Disodiumâ€Enhanced <scp>MRI</scp> : Toward Better Sensitivity and Simplicity. Journal of Magnetic Resonance Imaging, 2022, 55, 493-506.	1.9	6
3	CT/MRI and CEUS LI-RADS Major Features Association with Hepatocellular Carcinoma: Individual Patient Data Meta-Analysis. Radiology, 2022, 302, 326-335.	3.6	32
4	Modifying <scp>Llâ€RADS</scp> on Gadoxetate Disodiumâ€Enhanced <scp>MRI</scp> : A Secondary Analysis of a Prospective Observational Study. Journal of Magnetic Resonance Imaging, 2022, 56, 399-412.	1.9	6
5	PEGylated amphiphilic polymeric manganese(<scp>ii</scp>) complexes as magnetic resonance angiographic agents. Journal of Materials Chemistry B, 2022, 10, 2204-2214.	2.9	9
6	New Liver MR Imaging Hallmarks for Small Hepatocellular Carcinoma Screening and Diagnosing in High-Risk Patients. Frontiers in Oncology, 2022, 12, 812832.	1.3	1
7	Standard diffusion-weighted, diffusion kurtosis and intravoxel incoherent motion MR imaging of the whole placenta: a pilot study of volumetric analysis. Annals of Translational Medicine, 2022, 10, 269-269.	0.7	2
8	Hyperpolarized carbon 13 MRI in liver diseases: Recent advances and future opportunities. Liver International, 2022, 42, 973-983.	1.9	7
9	Predicting microvascular invasion in hepatocellular carcinoma: A dualâ€institution study on gadoxetate disodiumâ€enhanced <scp>MRI</scp> . Liver International, 2022, 42, 1158-1172.	1.9	30
10	Quantitative measurements of esophageal varices using computed tomography for prediction of severe varices and the risk of bleeding: a preliminary study. Insights Into Imaging, 2022, 13, 47.	1.6	2
11	Computed Tomography-Based Texture Features for the Risk Stratification of Portal Hypertension and Prediction of Survival in Patients With Cirrhosis: A Preliminary Study. Frontiers in Medicine, 2022, 9, 863596.	1.2	5
12	Noninvasive imaging of hepatic dysfunction: A state-of-the-art review. World Journal of Gastroenterology, 2022, 28, 1625-1640.	1.4	4
13	Comparison of a preoperative MR-based recurrence risk score versus the postoperative score and four clinical staging systems in hepatocellular carcinoma: a retrospective cohort study. European Radiology, 2022, 32, 7578-7589.	2.3	5
14	Providing higher value care for hepatocellular carcinoma rather than diagnosis: What can current radiologists do?. World Journal of Gastrointestinal Surgery, 2022, 14, 525-527.	0.8	0
15	Profiling hepatocellular carcinoma aggressiveness with contrast-enhanced ultrasound and gadoxetate disodium-enhanced MRI: An intra-individual comparative study based on the Liver Imaging Reporting and Data System. European Journal of Radiology, 2022, 154, 110397.	1.2	4
16	Prognostic implications of <scp>CT</scp> / <scp>MRI Llâ€RADS</scp> in hepatocellular carcinoma: State of the art and future directions. Liver International, 2022, 42, 2131-2144.	1.9	8
17	Use of computed tomography for distinguishing heterotopic pancreas from gastrointestinal stromal tumor and leiomyoma. Abdominal Radiology, 2021, 46, 168-178.	1.0	6
18	LI-RADS category 5 hepatocellular carcinoma: preoperative gadoxetic acid–enhanced MRI for early recurrence risk stratification after curative resection. European Radiology, 2021, 31, 2289-2302.	2.3	27

#	Article	IF	CITATIONS
19	Joint prediction and time estimation of COVID-19 developing severe symptoms using chest CT scan. Medical Image Analysis, 2021, 67, 101824.	7.0	58
20	Potential role of imaging for assessing acute pancreatitis-induced acute kidney injury. British Journal of Radiology, 2021, 94, 20200802.	1.0	5
21	Stool-based Xpert MTB/RIF Ultra assay as a tool for detecting pulmonary tuberculosis in children with abnormal chest imaging: A prospective cohort study. Journal of Infection, 2021, 82, 84-89.	1.7	16
22	Diagnosis of LI-RADS M lesions on gadoxetate-enhanced MRI: identifying cholangiocarcinoma-containing tumor with serum markers and imaging features. European Radiology, 2021, 31, 3638-3648.	2.3	15
23	Intrahepatic cholangiocarcinoma: MRI texture signature as predictive biomarkers of immunophenotyping and survival. European Radiology, 2021, 31, 3661-3672.	2.3	20
24	Hypergraph learning for identification of COVID-19 with CT imaging. Medical Image Analysis, 2021, 68, 101910.	7.0	56
25	COVID-19-associated coagulopathy: thromboembolism prophylaxis and poor prognosis in ICU. Experimental Hematology and Oncology, 2021, 10, 6.	2.0	12
26	Association of D-dimer elevation with inflammation and organ dysfunction in ICU patients with COVID-19 in Wuhan, China: a retrospective observational study. Aging, 2021, 13, 4794-4810.	1.4	9
27	Combining initial chest CT with clinical variables in differentiating coronavirus disease 2019 (COVID-19) pneumonia from influenza pneumonia. Scientific Reports, 2021, 11, 6422.	1.6	2
28	Large-scale screening to distinguish between COVID-19 and community-acquired pneumonia using infection size-aware classification. Physics in Medicine and Biology, 2021, 66, 065031.	1.6	233
29	The effectiveness of continuous renal replacement therapy in critical COVID-19 patients with cytokine release syndrome: a retrospective, multicenter, descriptive study from Wuhan, China. Aging, 2021, 13, 9243-9252.	1.4	5
30	Tetraphenylethylene-conjugated polycation covered iron oxide nanoparticles for magnetic resonance/optical dual-mode imaging. International Journal of Energy Production and Management, 2021, 8, rbab023.	1.9	10
31	External validation study of the 8th edition of the American Joint Committee on Cancer staging system for perihilar cholangiocarcinoma: a single-center experience in China and proposal for simplification. Journal of Gastrointestinal Oncology, 2021, 12, 806-818.	0.6	2
32	Macrotrabecular-massive hepatocellular carcinoma: imaging identification and prediction based on gadoxetic acid–enhanced magnetic resonance imaging. European Radiology, 2021, 31, 7696-7704.	2.3	23
33	Container CT scanner: a solution for modular emergency radiology department during the COVID-19 pandemic. Diagnostic and Interventional Radiology, 2021, 27, 350-353.	0.7	2
34	Development and validation of preoperative magnetic resonance imaging-based survival predictive nomograms for patients with perihilar cholangiocarcinoma after radical resection: A pilot study. European Journal of Radiology, 2021, 138, 109631.	1.2	10
35	Development and validation of MRIâ€based deep learning models for prediction of microsatellite instability in rectal cancer. Cancer Medicine, 2021, 10, 4164-4173.	1.3	29
36	Prediction of Remnant Liver Regeneration after Right Hepatectomy in Patients with Hepatocellular Carcinoma Using Preoperative CT Texture Analysis and Clinical Features. Contrast Media and Molecular Imaging, 2021, 2021, 1-8.	0.4	3

#	Article	IF	CITATIONS
37	Secondary infection in severe and critical COVID-19 patients in China: a multicenter retrospective study. Annals of Palliative Medicine, 2021, 10, 8557-8570.	0.5	25
38	Elevated Pancreatic Enzymes in ICU Patients With COVID-19 in Wuhan, China: A Retrospective Study. Frontiers in Medicine, 2021, 8, 663646.	1.2	14
39	Role of noninvasive imaging in the evaluation of intrahepatic cholangiocarcinoma: from diagnosis and prognosis to treatment response. Expert Review of Gastroenterology and Hepatology, 2021, 15, 1267-1279.	1.4	7
40	CT-derived quantitative liver volumetric parameters for prediction of severe esophageal varices and the risk of first variceal hemorrhage. European Journal of Radiology, 2021, 144, 109984.	1.2	9
41	Insight into gastrointestinal heterotopic pancreas: imaging evaluation and differential diagnosis. Insights Into Imaging, 2021, 12, 144.	1.6	10
42	Coagulation dysfunction in ICU patients with coronavirus disease 2019 in Wuhan, China: a retrospective observational study of 75 fatal cases. Aging, 2021, 13, 1591-1607.	1.4	3
43	Predictive Value of Metabolic Parameters Derived From F-FDG PET/CT for Microsatellite Instability in Patients With Colorectal Carcinoma. Frontiers in Immunology, 2021, 12, 724464.	2.2	1
44	Radiomics in hepatocellular carcinoma: A state-of-the-art review. World Journal of Gastrointestinal Oncology, 2021, 13, 1599-1615.	0.8	17
45	Predictive Value of Metabolic Parameters Derived From 18F-FDG PET/CT for Microsatellite Instability in Patients With Colorectal Carcinoma. Frontiers in Immunology, 2021, 12, 724464.	2.2	12
46	Integration of PEG-conjugated gadolinium complex and superparamagnetic iron oxide nanoparticles as <i>T</i> 1– <i>T</i> 2 dual-mode magnetic resonance imaging probes. International Journal of Energy Production and Management, 2021, 8, rbab064.	1.9	11
47	A Bounding Box-Based Radiomics Model for Detecting Occult Peritoneal Metastasis in Advanced Gastric Cancer: A Multicenter Study. Frontiers in Oncology, 2021, 11, 777760.	1.3	7
48	Noninvasive prediction of HCC with progenitor phenotype based on gadoxetic acid-enhanced MRI. European Radiology, 2020, 30, 1232-1242.	2.3	28
49	Differential Diagnosis of Nonhypervascular Pancreatic Neuroendocrine Neoplasms From Pancreatic Ductal Adenocarcinomas, Based on Computed Tomography Radiological Features and Texture Analysis. Academic Radiology, 2020, 27, 332-341.	1.3	16
50	Consensus report from the 8th International Forum for Liver Magnetic Resonance Imaging. European Radiology, 2020, 30, 370-382.	2.3	55
51	Computed Tomographic Portography with Esophageal Variceal Measurements in the Evaluation of Esophageal Variceal Severity and Assessment of Esophageal Variceal Volume Efficacy. Academic Radiology, 2020, 27, 528-535.	1.3	6
52	Improved Display of Hepatic Arterial Anatomy Using Differential Subsampling With Cartesian Ordering (DISCO) With Gadoxetic Acidâ€Enhanced MRI: Comparison With Single Arterial Phase MRI and Computed Tomographic Angiography. Journal of Magnetic Resonance Imaging, 2020, 51, 1766-1776.	1.9	6
53	Bioactive iron oxide nanoparticles suppress osteoclastogenesis and ovariectomy-induced bone loss through regulating the TRAF6-p62-CYLD signaling complex. Acta Biomaterialia, 2020, 103, 281-292.	4.1	38
54	Can LI-RADS imaging features at gadoxetic acid-enhanced MRI predict aggressive features on pathology of single hepatocellular carcinoma?. European Journal of Radiology, 2020, 132, 109312.	1.2	34

#	Article	IF	CITATIONS
55	Machine learning: an approach to preoperatively predict PD-1/PD-L1 expression and outcome in intrahepatic cholangiocarcinoma using MRI biomarkers. ESMO Open, 2020, 5, e000910.	2.0	38
56	Deep Convolutional Neural Network Based on Computed Tomography Images for the Preoperative Diagnosis of Occult Peritoneal Metastasis in Advanced Gastric Cancer. Frontiers in Oncology, 2020, 10, 601869.	1.3	16
57	A Quantitative and Radiomics approach to monitoring ARDS in COVID-19 patients based on chest CT: a retrospective cohort study. International Journal of Medical Sciences, 2020, 17, 1773-1782.	1.1	21
58	Survival analysis of patients with stage T2a and T2b perihilar cholangiocarcinoma treated with radical resection. BMC Cancer, 2020, 20, 849.	1.1	5
59	Prognosticators of intravoxel incoherent motion (IVIM) MRI for adverse maternal and neonatal clinical outcomes in patients with placenta accreta spectrum disorders. Translational Andrology and Urology, 2020, 9, 258-266.	0.6	8
60	A New Diagnostic Criterion with Gadoxetic Acid-Enhanced MRI May Improve the Diagnostic Performance for Hepatocellular Carcinoma. Liver Cancer, 2020, 9, 414-425.	4.2	9
61	CT Manifestations and Clinical Characteristics of 1115 Patients with Coronavirus Disease 2019 (COVID-19): A Systematic Review and Meta-analysis. Academic Radiology, 2020, 27, 910-921.	1.3	60
62	Radiomics in liver diseases: Current progress and future opportunities. Liver International, 2020, 40, 2050-2063.	1.9	70
63	Assessing Liver Function in Liver Tumors Patients: The Performance of T1 Mapping and Residual Liver Volume on Gd-EOBDTPA-Enhanced MRI. Frontiers in Medicine, 2020, 7, 215.	1.2	5
64	Preoperative prediction of hepatocellular carcinoma with highly aggressive characteristics using quantitative parameters derived from hepatobiliary phase MR images. Annals of Translational Medicine, 2020, 8, 85-85.	0.7	11
65	Differentiation combined hepatocellular and cholangiocarcinoma from intrahepatic cholangiocarcinoma based on radiomics machine learning. Annals of Translational Medicine, 2020, 8, 119-119.	0.7	38
66	Chest CT manifestations of new coronavirus disease 2019 (COVID-19): a pictorial review. European Radiology, 2020, 30, 4381-4389.	2.3	1,009
67	Clinical course and risk factors for mortality of adult inpatients with COVID-19 in Wuhan, China: a retrospective cohort study. Lancet, The, 2020, 395, 1054-1062.	6.3	21,698
68	The Battle Against Coronavirus Disease 2019 (COVID-19): Emergency Management and Infection Control in a Radiology Department. Journal of the American College of Radiology, 2020, 17, 710-716.	0.9	110
69	Two-dimensional shear wave elastography for significant liver fibrosis in patients with chronic hepatitis B: A systematic review and meta-analysis. European Journal of Radiology, 2020, 124, 108839.	1.2	11
70	Evaluating the correlation of the impairment between skeletal muscle and heart using MRI in a spontaneous type 2 diabetes mellitus rhesus monkey model. Acta Diabetologica, 2020, 57, 673-679.	1.2	3
71	Characteristic CT findings distinguishing 2019 novel coronavirus disease (COVID-19) from influenza pneumonia. European Radiology, 2020, 30, 4910-4917.	2.3	88
72	Multiparametric radiomics nomogram may be used for predicting the severity of esophageal varices in cirrhotic patients. Annals of Translational Medicine, 2020, 8, 186-186.	0.7	8

#	Article	IF	CITATIONS
73	Use of Radiomics to Improve Diagnostic Performance of PI-RADS v2.1 in Prostate Cancer. Frontiers in Oncology, 2020, 10, 631831.	1.3	17
74	Dual-Sampling Attention Network for Diagnosis of COVID-19 From Community Acquired Pneumonia. IEEE Transactions on Medical Imaging, 2020, 39, 2595-2605.	5.4	293
75	Independent Risk Factors of Early Recurrence After Curative Resection for Perihilar Cholangiocarcinoma: Adjuvant Chemotherapy May Be Beneficial in Early Recurrence Subgroup. Cancer Management and Research, 2020, Volume 12, 13111-13123.	0.9	5
76	Value of intravoxel incoherent motion in detecting and staging liver fibrosis: A meta-analysis. World Journal of Gastroenterology, 2020, 26, 3304-3317.	1.4	7
77	Radiomics of rectal cancer for predicting distant metastasis and overall survival. World Journal of Gastroenterology, 2020, 26, 5008-5021.	1.4	22
78	Elastography for Longitudinal Assessment of Liver Fibrosis after Antiviral Therapy: A Review. Journal of Clinical and Translational Hepatology, 2020, 8, 1-9.	0.7	5
79	Intravoxel incoherent motion diffusion-weighted imaging for assessment of histologic grade of hepatocellular carcinoma: comparison of three methods for positioning region of interest. European Radiology, 2019, 29, 535-544.	2.3	34
80	Role of medical imaging for immune checkpoint blockade therapy: From response assessment to prognosis prediction. Cancer Medicine, 2019, 8, 5399-5413.	1.3	15
81	Iron oxide nanoparticles promote vascular endothelial cells survival from oxidative stress by enhancement of autophagy. International Journal of Energy Production and Management, 2019, 6, 221-229.	1.9	21
82	Hepatocellular carcinoma: Can LI-RADS v2017 with gadoxetic-acid enhancement magnetic resonance and diffusion-weighted imaging improve diagnostic accuracy?. World Journal of Gastroenterology, 2019, 25, 622-631.	1.4	21
83	Effects of aging and menopause on pancreatic fat fraction in healthy women population. Medicine (United States), 2019, 98, e14451.	0.4	10
84	Preoperative Radiomic Approach to Evaluate Tumor-Infiltrating CD8+ T Cells in Hepatocellular Carcinoma Patients Using Contrast-Enhanced Computed Tomography. Annals of Surgical Oncology, 2019, 26, 4537-4547.	0.7	62
85	Gadoxetate acid disodium-enhanced MRI: Multiple arterial phases using differential sub-sampling with cartesian ordering (DISCO) may achieve more optimal late arterial phases than the single arterial phase imaging. Magnetic Resonance Imaging, 2019, 61, 116-123.	1.0	10
86	Hepatocellular carcinoma: radiomics nomogram on gadoxetic acid-enhanced MR imaging for early postoperative recurrence prediction. Cancer Imaging, 2019, 19, 22.	1.2	90
87	Diffusion kurtosis imaging (DKI) of hepatocellular carcinoma: correlation with microvascular invasion and histologic grade. Quantitative Imaging in Medicine and Surgery, 2019, 9, 590-602.	1.1	42
88	IVIM improves preoperative assessment of microvascular invasion in HCC. European Radiology, 2019, 29, 5403-5414.	2.3	63
89	Iron oxide nanoparticles promote macrophage autophagy and inflammatory response through activation of toll-like Receptor-4 signaling. Biomaterials, 2019, 203, 23-30.	5.7	102
90	Man or machine? Prospective comparison of the version 2018 EASL, LI-RADS criteria and a radiomics model to diagnose hepatocellular carcinoma. Cancer Imaging, 2019, 19, 84.	1.2	36

#	Article	IF	CITATIONS
91	Two-dimensional Texture Analysis Based on CT Images to Differentiate Pancreatic Lymphoma and Pancreatic Adenocarcinoma: A Preliminary Study. Academic Radiology, 2019, 26, e189-e195.	1.3	29
92	Texture analysis on gadoxetic acid enhanced-MRI for predicting Ki-67 status in hepatocellular carcinoma: A prospective study. Chinese Journal of Cancer Research: Official Journal of China Anti-Cancer Association, Beijing Institute for Cancer Research, 2019, 31, 806-817.	0.7	31
93	Quantification of pancreatic fat with dual-echo imaging at 3.0-T MR in clinical application: how do the corrections for T1 and T2* relaxation effect work and simplified correction strategy. Acta Radiologica, 2018, 59, 1021-1028.	0.5	4
94	Non-invasive in vivo Imaging Grading of Liver Fibrosis. Journal of Clinical and Translational Hepatology, 2018, 6, 1-10.	0.7	22
95	2D/3D CMR tissue tracking versus CMR tagging in the assessment of spontaneous T2DM rhesus monkeys with isolated diastolic dysfunction. BMC Medical Imaging, 2018, 18, 47.	1.4	9
96	Noninvasive imaging of hepatocellular carcinoma: From diagnosis to prognosis. World Journal of Gastroenterology, 2018, 24, 2348-2362.	1.4	109
97	The Value of Modified Renal Rim Grade in Predicting Acute Kidney Injury Following Severe Acute Pancreatitis. Journal of Computer Assisted Tomography, 2018, 42, 680-687.	0.5	5
98	Intrahepatic cholangiocarcinoma in the setting of HBV-related cirrhosis: Differentiation with hepatocellular carcinoma by using Intravoxel incoherent motion diffusion-weighted MR imaging. Oncotarget, 2018, 9, 7975-7983.	0.8	19
99	Evaluation of extrapancreatic inflammation on abdominal computed tomography as an early predictor of organ failure in acute pancreatitis as defined by the revised Atlanta classification. Medicine (United) Tj ETQq	100 7 843	14 1g BT /Ove
100	Liver fibrosis: in vivo evaluation using intravoxel incoherent motion-derived histogram metrics with histopathologic findings at 3.0 T. Abdominal Radiology, 2017, 42, 2855-2863.	1.0	14
101	Gadoxetic acid disodium–enhanced magnetic resonance imaging outperformed multidetector computed tomography in diagnosing small hepatocellular carcinoma: A metaâ€analysis. Liver Transplantation, 2017, 23, 1505-1518.	1.3	71
102	Liver fibrosis staging with diffusion-weighted imaging: a systematic review and meta-analysis. Abdominal Radiology, 2017, 42, 490-501.	1.0	47
103	Accuracy of contrast-enhanced ultrasound compared with conventional ultrasound in acute pancreatitis: Diagnosis and complication monitoring. Experimental and Therapeutic Medicine, 2016, 12, 3189-3194.	0.8	10
104	Control of the interparticle spacing in superparamagnetic iron oxide nanoparticle clusters by surface ligand engineering. Chinese Physics B, 2016, 25, 077504.	0.7	4
105	The effect of neighbor distance of magnetic nanoparticle clusters on magnetic resonance relaxation properties. Science Bulletin, 2016, 61, 1023-1030.	4.3	16
106	Negatively Charged Magnetite Nanoparticle Clusters as Efficient MRI Probes for Dendritic Cell Labeling and In Vivo Tracking. Advanced Functional Materials, 2015, 25, 3581-3591.	7.8	43
107	Preoperative Evaluation of the Histological Grade of Hepatocellular Carcinoma with Diffusion-Weighted Imaging: A Meta-Analysis. PLoS ONE, 2015, 10, e0117661.	1.1	27
108	Multivalent manganese complex decorated amphiphilic dextran micelles as sensitive MRI probes. Journal of Materials Chemistry B, 2015, 3, 1470-1473.	2.9	26

#	Article	IF	CITATIONS
109	Multifunctional dextran micelles as drug delivery carriers and magnetic resonance imaging probes. Science Bulletin, 2015, 60, 1272-1280.	4.3	36
110	Superparamagnetic MRI probes for inÂvivo tracking of dendritic cell migration with a clinical 3ÂT scanner. Biomaterials, 2015, 58, 63-71.	5.7	39
111	Correlation analysis of computed tomography imaging score with the presence of acute kidney injury in severe acute pancreatitis. Abdominal Imaging, 2015, 40, 1241-1247.	2.0	5
112	Magnetic Resonance Imaging for Monitoring of Magnetic Polyelectrolyte Capsule In Vivo Delivery. BioNanoScience, 2014, 4, 59-70.	1.5	20
113	Delivery of siRNA by MRI-visible nanovehicles to overcome drug resistance in MCF-7/ADR human breast cancer cells. Biomaterials, 2014, 35, 9495-9507.	5.7	67
114	Amphiphilic starlike dextran wrapped superparamagnetic iron oxide nanoparticle clsuters as effective magnetic resonance imaging probes. Biomaterials, 2013, 34, 1193-1203.	5.7	89
115	Near-infrared fluorescent amphiphilic polycation wrapped magnetite nanoparticles as multimodality probes. Science Bulletin, 2012, 57, 4012-4018.	1.7	14
116	Rigid Mn(ii) chelate as efficient MRI contrast agent for vascular imaging. Dalton Transactions, 2012, 41, 14480.	1.6	51
117	Magnetic resonance tumor targeting imaging using gadolinium labeled human telomerase reverse transcriptase antisense probes. Cancer Science, 2012, 103, 1434-1439.	1.7	6
118	Noninvasive Quantification of Pancreatic Fat in Healthy Male Population Using Chemical Shift Magnetic Resonance Imaging. Pancreas, 2011, 40, 295-299.	0.5	46
119	Gadolinium-labeled peptide dendrimers with controlled structures as potential magnetic resonance imaging contrast agents. Biomaterials, 2011, 32, 7951-7960.	5.7	98
120	Magnetic resonance imaging probes for labeling of chondrocyte cells. Journal of Materials Science: Materials in Medicine, 2011, 22, 601-606.	1.7	22
121	Multifunctional gadolinium-based dendritic macromolecules as liver targeting imaging probes. Biomaterials, 2011, 32, 2575-2585.	5.7	65
122	Low molecular weight alkyl-polycation wrapped magnetite nanoparticle clusters as MRI probes for stem cell labeling and in vivo imaging. Biomaterials, 2011, 32, 528-537.	5.7	126
123	Self-Assembly of SiO ₂ /Gd-DTPA-Polyethylenimine Nanocomposites as Magnetic Resonance Imaging Probes. Journal of Nanoscience and Nanotechnology, 2010, 10, 540-548.	0.9	24
124	Functional <scp>L</scp> â€Lysine Dendritic Macromolecules as Liverâ€Imaging Probes. Macromolecular Bioscience, 2009, 9, 1227-1236.	2.1	55
125	Amphiphilic dextran/magnetite nanocomposites as magnetic resonance imaging probes. Science Bulletin, 2009, 54, 2925-2933.	1.7	15
126	Manganese ferrite nanoparticle micellar nanocomposites as MRI contrast agent for liver imaging. Biomaterials, 2009, 30, 2919-2928.	5.7	325

#	Article	IF	CITATIONS
127	Self-Assembly of Magnetite Nanocrystals with Amphiphilic Polyethylenimine: Structures and Applications in Magnetic Resonance Imaging. Journal of Nanoscience and Nanotechnology, 2009, 9, 378-385.	0.9	49